

## WHY ARE PULSAR PLANETS RARE?

REBECCA G. MARTIN, MARIO LIVIO, AND DIVYA PALANISWAMY

Department of Physics and Astronomy, University of Nevada, Las Vegas, 4505 South Maryland Parkway, Las Vegas, NV 89154, USA  
*Draft version September 22, 2016*

### ABSTRACT

Pulsar timing observations have revealed planets around only a few pulsars. We suggest that the rarity of these planets is due mainly to two effects. First, we show that the most likely formation mechanism requires the destruction of a companion star. Only pulsars with a suitable companion (with an extreme mass ratio) are able to form planets. Second, while a dead zone (a region of low turbulence) in the disk is generally thought to be essential for planet formation, it is most probably rare in disks around pulsars because of the irradiation from the pulsar. The irradiation strongly heats the inner parts of the disk pushing the inner boundary of the dead zone out. We suggest that the rarity of pulsar planets can be explained by the low probability for these two requirements – a very low-mass companion and a dead zone – to be satisfied.

*Subject headings:* accretion, accretion disks – protoplanetary disks – planets and satellites: formation – pulsars: general

### 1. INTRODUCTION

There are currently five exoplanets in three planetary systems that have been detected through pulsar timing to be orbiting pulsars, rapidly rotating highly magnetized neutron stars (Lorimer 2008). The masses and semi-major axes of these planets are shown in Table 1 and plotted in the blue points in Fig. 1. The first planets to be discovered (and immediately confirmed) outside of our solar system were in fact found around the pulsar PSR B1257+12 (Wolszczan & Frail 1992; Wolszczan 1994, 2012). This pulsar has three very close-in planets. The outer two planets are coplanar within 6° and all three have low eccentricity, implying a disk origin (Konacki & Wolszczan 2003). The outer two planets are close to a 3:2 mean-motion resonance. This suggests that the planets did not form at their current location but instead probably migrated in from farther out, possibly through a gas disk (e.g. Terquem & Papaloizou 2007). A planet has also been observed around the pulsar PSR J1719–1438. This planet has a mass similar to Jupiter but a radius of less than about 40% (Bailes et al. 2011). It is thought to be an ultra-low mass white dwarf companion that has narrowly avoided complete destruction (van Haaften et al. 2012). Finally, a planet has been detected around the pulsar PSR B1620–26 (Backer et al. 1993; Sigurdsson et al. 2003). This pulsar is a part of a binary star system with a white dwarf and the planet is in a circumbinary orbit. The most likely formation mechanism for this pulsar is that a star and planet were captured by the pulsar, whose original companion was ejected into space and lost (Rasio 1994; Ford et al. 2000). Thus, this planet probably did not form around the pulsar. All of the pulsar planets found so far are around old millisecond pulsars (MSPs) that are thought to have been spun up by accretion of matter from a companion star (e.g. Alpar et al. 1982; Bhattacharya & van den Heuvel 1991).

The precision of the pulsar timing allows detections of very low mass bodies outside of the solar system (Wolszczan 1994, 1997). The lower limit on the mass of an observable planet is

$$M_{\text{planet}} \sin(i) \approx 0.90 \left( \frac{\tau_{\text{pl}}}{1 \text{ ms}} \right) \left( \frac{a}{1 \text{ AU}} \right)^{-1} M_{\oplus} \quad (1)$$

(Wolszczan 1997), where  $M_{\oplus}$  is the mass of the Earth,  $\tau_{\text{pl}}$  is the measured timing residual amplitude,  $a$  is the or-

**Table 1**

Mass and semi-major axis of planets observed around pulsars

Planet	$M_{\text{planet}}$	$a/\text{AU}$
PSR B1257+12 A	0.02 $M_{\oplus}$	0.19
PSR B1257+12 B	4.3 $M_{\oplus}$	0.36
PSR B1257+12 C	3.9 $M_{\oplus}$	0.46
PSR J1719-1438 b	1 $M_{\text{J}}$	0.004
PSR B1620–26 b	2.5 $M_{\text{J}}$	23

bit semi-major axis and  $i$  is the orbital inclination (e.g. Thorsett & Phillips 1992; Blandford 1993; Bailes et al. 1993; Wolszczan 1997). The pulsar is assumed to have a mass  $M_{\text{p}} = 1.35 M_{\odot}$ . We show the detectability limits in Figure 1 for timing residuals of 1  $\mu\text{s}$  (applicable to MSPs) and 1 ms (applicable to normal pulsars) and compare to objects in the solar system. Jovian planets are easily detectable around a normal slow pulsar, whereas terrestrial planets, down to the size of large asteroids, can be found in the timing residual of a MSP.

Despite the successes in finding planets around pulsars and the precision offered, pulsar planets are rare (e.g. Bailes 1996; Bell et al. 1997). In particular, the survey of Kerr et al. (2015) of 151 young pulsars revealed no planets. Similarly, the Australian Telescope National Facility (ATNF) pulsar catalogue<sup>1</sup> currently contains 2536 pulsars of which 436 are MSPs with spin period < 10 ms (Manchester et al. 2005). Less than 1% of observed MSPs have a planetary mass companion.

In Section 2 we discuss different potential pulsar planet formation models and find that the most likely place for a pulsar planet to form is in a disk formed by the destruction of a binary companion. In Section 3 we discuss the probability for the formation of an extreme mass ratio binary required for pulsar planet formation. In addition, most planet formation scenarios require the presence of a “dead zone” in the protoplanetary disk. This is a quiescent region where the magneto-rotational instability (MRI) is unable to drive turbulence and angular momentum transport (e.g. Gammie 1996; Gammie & Menou 1998; Currie & Hansen 2007). The dead zone is thought to be a necessary com-

<sup>1</sup> <http://www.atnf.csiro.au/people/pulsar/psrcat/>

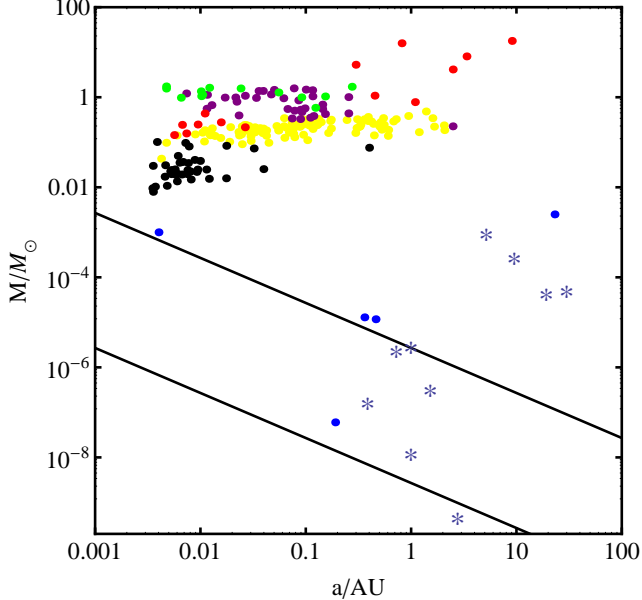


**Figure 1.** Pulsar companion mass and semi-major axis. The mass is the median mass assuming an orbital inclination of  $i = 60^\circ$ . The assumed primary pulsar mass is  $1.35 M_\odot$ . The companions are planets (blue points), main-sequence stars (red points), ultra low-mass (black points), neutron stars (green points), CO or ONeMg white dwarfs (purple points) or helium white dwarfs (yellow points). The blue stars show the 8 planets in the solar system, the Moon, and the asteroid Ceres. The solid lines show the detection limit for timing residuals of  $1 \mu\text{s}$  (lower line, applicable for millisecond pulsars) and  $1 \text{ ms}$  (upper line, applicable for normal slow pulsars) found with equation (1).

ponent for planet formation for several reasons. First, it provides a quiescent region where solids can settle to the midplane (e.g. Youdin & Shu 2002; Youdin & Lithwick 2007; Zsom et al. 2011). Second, it allows planetesimals to form (e.g. Chambers 2010; Bai & Stone 2010; Youdin 2011). Finally, it slows the rate of low-mass planet migration, preventing them from falling into the star (e.g. Ward 1997; Thommes 2005; Matsumura & Pudritz 2006). In Section 4 we consider whether a dead zone can form in a disk around a pulsar. We discuss and summarize our results in Sections 5 and 6.

## 2. PULSAR PLANET FORMATION MODELS

There are several proposed mechanisms for planet formation around a pulsar (e.g. Podsiadlowski 1993, 1995). In this section we discuss each in turn.

### 2.1. Planets that survive the supernova?

It is worth considering whether it is possible (at least in principle) for planets to form in the usual way, in a protoplanetary disk around a young (massive) star, and survive the pulsar formation process (e.g. Bailes et al. 1991). However, there is some doubt as to whether planets can even form around a star massive enough to become a pulsar. There is a strong decline in the probability of a star hosting a giant planet for mass greater than  $3 M_\odot$  (e.g. Kennedy & Kenyon 2008). Currently, the most massive star to have a detected planet is  $3 M_\odot$  (Han et al. 2014). This dearth of planets around massive stars could be the result of several factors. First, there is intense UV radiation from the star that can rapidly destroy the disk. Second, the lifetime of the star is much shorter. We should note, however, that selection effects may be important since

the planets (if they exist) would probably be impossible to detect. Because the star is more massive and brighter than a low mass star, neither the transit method nor the radial velocity method is sensitive enough to detect a planet.

Supposing that such planets can still form, then there are several conditions that must be met in order for them to survive the death of the star. The orbital radii of the planets must be larger than about 4 AU in order to survive being engulfed during the red-giant phase. In the supernova explosion, half of the mass of the system is ejected. In order for planets to survive, the explosion must be asymmetric. The asymmetry results in a velocity kick to the newly formed pulsar that must be in a similar direction to the motion of the planet at the time of the supernova (Blaauw 1961; Bhattacharya & van den Heuvel 1991). Planets that survive would be expected to be in eccentric orbits at orbital radii of at least a few AU (e.g. Thorsett et al. 1993).

This mechanism is unlikely to form a system with more than one planet (if any). For three planets to survive this process is almost certainly impossible and so the planets around PSR B1257+12 formed after the pulsar. Furthermore, the two other known pulsar planets most likely did not form in this way since PSR B1620-26 is a circumbinary planet and PSR J1719-1438 is extremely close to its host star. None of the known pulsar planets formed in this way and we suggest that the probability for planets to form in this scenario is negligible.

### 2.2. Supernova fallback disk?

When a pulsar forms in a supernova, most of the material of the star is ejected. However, some material can fall back towards the newly formed pulsar if it does not attain the escape velocity or if it is pushed back during the early hydrodynamical mixing phase (e.g. Colgate 1971; Chevalier 1989; Bailes et al. 1991). Estimates of the total mass that can form the fall back disk are in the range  $0.001-0.1 M_\odot$  (e.g. Lin et al. 1991; Menou et al. 2001). This is similar to the masses observed in protoplanetary disks around young stars that lie in the range  $0.001-0.1 M_\star$  (e.g. Williams & Cieza 2011), where  $M_\star$  is the mass of the host star. However, the angular momentum of the fallback disk may be very different. Recently, Perna et al. (2014) considered the formation of a supernova fallback disk around neutron stars (and black holes) with numerical simulations of supernova explosions. They found that if magnetic torques play a role in angular momentum transport, then supernova fallback disks do not form around neutron stars. Any material that falls back has too little angular momentum to orbit the neutron star even once. However, formation can occur when the magnetic torques are negligible. This requires the energy of the explosion to be finely tuned so that the fall back mass would on one hand not cause the neutron star to collapse to a black hole, but on the other would be sufficient to form a disk. Perna et al. (2014) found a typical fallback mass of  $0.08 M_\odot$  with the maximum specific angular momentum of the material  $\leq 10^{17} \text{ cm}^2 \text{ s}^{-1}$ .

We can calculate the circularization radius for such a disk. The radius of a ring of material with a given specific angular momentum,  $j$ , is

$$R_{\text{circ}} = \frac{j^2}{GM_p}, \quad (2)$$

where  $M_p$  is the mass of the pulsar. For typical parameters

this is

$$R_{\text{circ}} = 5.4 \times 10^7 \left( \frac{j}{10^{17} \text{ erg s}} \right)^2 \left( \frac{M_p}{1.4 M_\odot} \right)^{-1} \text{ cm.} \quad (3)$$

The upper limit to the total angular momentum of such a disk is estimated to be

$$J = 2 \times 10^{49} \left( \frac{M_d}{0.1 M_\odot} \right) \left( \frac{j}{10^{17} \text{ erg s}} \right) \text{ erg s,} \quad (4)$$

where  $M_d$  is the mass of the disk. This is in line with estimates by Phinney & Hansen (1993) and Menou et al. (2001). A simple estimate for the lifetime of such a disk is the viscous timescale

$$\tau_v = \frac{R^2}{\nu}, \quad (5)$$

where the viscosity is

$$\nu = \alpha \left( \frac{H}{R} \right)^2 R^2 \Omega, \quad (6)$$

$H/R$  is the disk aspect ratio,  $\Omega = \sqrt{GM_p/R^3}$  is the Keplerian angular frequency and  $\alpha$  is the Shakura & Sunyaev (1973) viscosity parameter. For typical values at the circularization radius we find

$$\tau_v(R_{\text{circ}}) = 2.8 \times 10^4 \left( \frac{\alpha}{0.01} \right)^{-1} \left( \frac{H/R}{0.01} \right)^{-2} \left( \frac{M_p}{1.4 M_\odot} \right)^{-2} \left( \frac{j}{10^{17} \text{ erg s}} \right)^3 \text{ s.} \quad (7)$$

The viscous disk spreads both inwards and outwards leading to a longer lifetime for larger radii. However, even an increase in this timescale by several orders of magnitude would not be sufficient for a reasonable timescale for planet formation. Even taking into account uncertainties in some of the physical parameters, if a supernova fallback disk does form, its lifetime is far too short for planet formation to occur.

Observations aimed at finding fallback disks around pulsars have not been successful (e.g. Wang et al. 2007). This, combined with the lack of observed planets around young pulsars (Kerr et al. 2015) suggests that planets do not form in a supernova fallback disk. The observed planets more likely formed during a later accretion phase that led to the spin up of the pulsar.

### 2.3. Destruction of a companion star

This model involves a close binary composed of a MSP (or its progenitor) and a low-mass main-sequence star or compact companion (e.g. Podsiadlowski et al. 1991; Stevens et al. 1992). The companion is losing mass through evaporation because it is being irradiated by the pulsar. If the evaporation timescale is shorter than the Kelvin–Helmholtz timescale the secondary responds adiabatically to the mass loss. The companion star fills its Roche lobe and is dynamically disrupted if its radius increases faster than the Roche-lobe radius (e.g. Benz et al. 1990). This is most likely to happen when the companion is fully convective or degenerate (e.g. for a low mass star the radius of the star is proportional to  $M^{-1/3}$ , where  $M$  is the mass of the star). The star is dynamically disrupted and forms a massive disk around the primary with a mass of around  $0.1 M_\odot$ .

In the specific case of the merger of two white dwarfs, the orbit shrinks due to gravitational radiation until the less massive white dwarf fills its Roche lobe. However, in this case,

there is some uncertainty whether the merger will lead to a type Ia supernova rather than to the formation of a pulsar (e.g. Livio 2000). It is most likely that a pulsar must be a component of the binary before the destruction of the companion.

During the dissolution of a companion star, the material forms a disk at a radius comparable to the initial separation of the binary, but then spreads out through viscous effects. Note that the disk formed is much larger than that expected from a supernova fallback disk. The total angular momentum of the disk is

$$J = 1.1 \times 10^{52} \left( \frac{M_d}{0.1 M_\odot} \right) \left( \frac{M_p}{1.4 M_\odot} \right)^{\frac{1}{2}} \left( \frac{a}{1 \text{ AU}} \right)^{\frac{1}{2}} \text{ erg s} \quad (8)$$

This is several orders of magnitude higher than the maximum estimate for the angular momentum of the supernova fallback disk given in equation (4). With the viscous timescale given by equation (5) and the viscosity in equation (6), at a radius of  $R = 1 \text{ AU}$ , we find the viscous timescale to be

$$\tau_v = 1.34 \times 10^5 \left( \frac{\alpha}{0.01} \right)^{-1} \left( \frac{H/R}{0.01} \right)^{-2} \left( \frac{M_p}{1.4 M_\odot} \right)^{-\frac{1}{2}} \left( \frac{R}{1 \text{ AU}} \right)^{\frac{3}{2}} \text{ yr.} \quad (9)$$

Since some material spreads outwards from its initial radius, the disk lifetime is longer than this. For example, material that reaches  $R = 5 \text{ AU}$  has a viscous timescale of over 1 Myr. This is similar to the disk lifetime for a protoplanetary disk around a young star (e.g. Williams & Cieza 2011). We therefore suggest that the destruction of a companion star is the most likely scenario for forming the planetary system around PSR B1257+12. The accretion rate is typically  $\dot{M} = M_d/\tau_v$  which is

$$\dot{M} = 6.64 \times 10^{-8} \left( \frac{\alpha}{0.01} \right) \left( \frac{H/R}{0.01} \right)^2 \left( \frac{M_d}{0.1 M_\odot} \right) \times \left( \frac{M_p}{1.4 M_\odot} \right)^{\frac{1}{2}} \left( \frac{R}{5 \text{ AU}} \right)^{-\frac{3}{2}} M_\odot \text{ yr}^{-1}. \quad (10)$$

This is similar to typical accretion rates observed around young T Tauri stars (e.g. Armitage et al. 2003; Calvet et al. 2004). Over time, as the mass of the disk decreases, the accretion rate also decreases. For a fully viscous disk, once the material has spread out into the inner regions, the disk can be modeled to be in a quasi-steady-state. In Section 4 we investigate the properties of this model further.

### 2.4. Evaporation of a companion

A companion star may be evaporated by the radiation from a pulsar (Fruchter et al. 1990; Bailes et al. 1991; Krolik 1991; Rasio et al. 1992; Tavani & Brookshaw 1992). The companion has to be almost, but not completely, evaporated by the pulsar leaving a remnant that is planet sized. This is thought to be the explanation for the planet in PSR J1719–1438. This mechanism is only capable of forming a single planet around a pulsar and so this scenario is unlikely to have been responsible for the planetary system around PSR B1257+12. The fine tuning required for this mechanism for planet formation means that this is probably a rare event. If the companion is completely evaporated and the planets form from that debris, then the formation is somewhat similar to that described in the previous Section 2.3. However, the disk formed in this man-

ner may have very little mass and so planet formation may be unlikely.

In summary, the most likely mechanisms for pulsar planet formation require a low mass companion to the pulsar. In the next Section we examine the parameters required to form an extreme mass ratio binary that is potentially capable of pulsar planet formation.

### 3. BINARY FORMATION

As we have shown in the previous section, planet formation around a pulsar requires a low mass binary companion. A massive star that ends its life as a neutron star has a mass in the approximate range  $9 - 25 M_{\odot}$  (Heger et al. 2003). The binary fraction of high mass stars may be quite high, up to 100% (e.g. Kratter & Matzner 2006; Mason et al. 2009). However, for pulsar planet formation, the binary companion must have a mass such that when it is accreted on to the pulsar it does not cause the latter to collapse to form a black hole. If the companion is a fully convective low mass main–sequence star, its mass is in the approximate range  $0.1 M_{\odot} \lesssim M_2 \lesssim 0.3 M_{\odot}$ . Alternatively, the companion may be a very low mass white dwarf, and the progenitor star would have to have a mass less than a solar mass. Observationally, the mass ratio distribution of binaries is dependent on the mass of the primary star (e.g. Bastian et al. 2010). The binary mass ratio distribution for high mass primary stars is not well constrained for low mass ratios,  $q \lesssim 0.1$ . However, for  $0.1 < q < 1$  the mass ratio distribution is relatively flat (e.g. Duchêne & Kraus 2013). Assuming that this extends to lower mass objects the probability of a binary forming with a mass ratio required to form pulsar planets  $q = M_2/M_1 < 0.1$  is  $\lesssim 10\%$ .

When the pulsar formed in a supernova explosion, an asymmetry in the explosion leads to a kick on the newly formed neutron star (e.g. Shklovskii 1970). If the supernova kick is too strong, the system does not remain bound (e.g. Brandt & Podsiadlowski 1995; Martin et al. 2009, 2010). The smaller the binary companion, the more likely the system is to become unbound. For a binary system that can form pulsar planets, we estimate that the probability of a bound orbit is  $\lesssim 10\%$  (see Figure 2 in Brandt & Podsiadlowski 1995).

In conclusion, we find that pulsar planet formation requires both an extreme mass ratio binary and for this binary to survive the supernova explosion that forms the pulsar. The probability of an extreme mass ratio binary forming and surviving the supernova is very small.

### 4. PULSAR DISK MODELS

The main difference between a protoplanetary disk around a young star and a disk around a pulsar is that the pulsar strongly irradiates the disk and provides an additional source of heating. We consider whether a dead zone forms in pulsar disks by considering the surface density and temperature structure of a disk around a pulsar.

The MRI drives turbulence within an accretion disk that transports angular momentum outwards allowing material to spiral inwards (e.g. Balbus & Hawley 1991). The MRI operates when the disk is sufficiently ionized, which requires a temperature greater than the critical value,  $T > T_{\text{crit}}$ . The value of the critical temperature is thought to be in the range  $800 - 1400$  K (e.g. Umebayashi & Nakano 1988; Zhu et al. 2010b). The disk temperature decreases with radius. For temperatures lower than the critical value, the disk is only fully MRI active if the surface density is sufficiently small,

$\Sigma < \Sigma_{\text{crit}}$ . If the surface density is larger than the critical value, a dead zone forms at the midplane and material only flows through the surface layers since these may be ionized by external sources. Cosmic rays ionize about  $200 \text{ g cm}^{-2}$  (e.g. Gammie 1996; Fromang et al. 2002). However, an MHD jet or a disk wind can sweep away the cosmic rays (e.g. Skilling & Strong 1976; Cesarsky & Volk 1978). Low–energy cosmic rays ionize more than higher energy cosmic rays (e.g. Lepp 1992) and these may be excluded from the disk by magnetic scattering. X-rays can only penetrate a much smaller surface density of around  $0.1 \text{ g cm}^{-2}$  (e.g. Matsumura & Pudritz 2003; Glassgold et al. 2004). Since there is some uncertainty as to the critical value for the surface density, we regard  $\Sigma_{\text{crit}}$  as a free parameter and consider different values in this work (see also Armitage et al. 2001; Zhu et al. 2009; Martin et al. 2012a,b).

A disk with a dead zone is not in a steady state, as material builds up there. The dead zone acts like a plug in the accretion flow and material can only flow through the surface layers with surface density,  $\Sigma_{\text{crit}}$ . This can result in a massive disk that is unstable to gravitational instability if the Toomre (1964) parameter becomes sufficiently small. This leads to gravitational turbulence that heats the disk and can potentially trigger the MRI in the dead zone. This causes an accretion outburst (e.g. Armitage et al. 2001; Zhu et al. 2010a; Martin & Lubow 2011, 2013, 2014). Around a young star, an accretion outburst accretes around  $0.1 M_{\odot}$ . Since this is the total mass of the disk around the pulsar and this material spreads out, outbursts are unlikely around pulsars. Thus we can consider just the location of a dead zone in a disk around a pulsar. We consider a quasi–steady–state disk model which assumes that the disk is fully turbulent for each accretion rate, but we determine when and where a dead zone exists.

#### 4.1. Inner edge of the dead zone

If a dead zone forms, the inner edge, closest to the star, is determined by where the temperature of the disk drops below the critical temperature,  $T < T_{\text{crit}}$ . In this section, we assume that in the inner parts of the disk, the temperature is dominated by the irradiation from the pulsar. The heating due to the irradiation is

$$Q_{\text{irr}} = \sigma T_{\text{irr}}^4 = \frac{L}{4\pi R^2} (1 - \beta) \cos \phi, \quad (11)$$

(e.g. Frank et al. 2002) where the albedo is  $\beta = 0.5$  and

$$\cos \phi = \frac{dH}{dR} - \frac{H}{R}. \quad (12)$$

The accretion luminosity is

$$L_{\text{acc}} = \frac{GM_{\text{p}}\dot{M}}{R_{\text{p}}}, \quad (13)$$

where  $\dot{M}$  is the accretion rate on to the pulsar. For typical values this is

$$L_{\text{acc}} = 3.1 \times 10^4 \left( \frac{\dot{M}}{10^{-8} M_{\odot} \text{ yr}^{-1}} \right) \left( \frac{M_{\text{p}}}{1.4 M_{\odot}} \right) \left( \frac{R_{\text{p}}}{10 \text{ km}} \right)^{-1} L_{\odot}. \quad (14)$$

However, this is limited by the Eddington luminosity,

$$L_{\text{EDD}} = 4.5 \times 10^4 \left( \frac{M_{\text{p}}}{1.4 M_{\odot}} \right) L_{\odot}. \quad (15)$$

Therefore, the luminosity in equation (11) is

$$L = \min(L_{\text{acc}}, L_{\text{EDD}}). \quad (16)$$

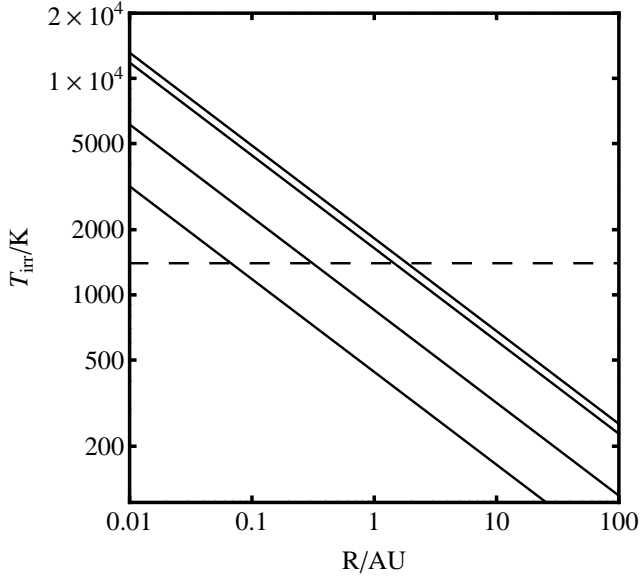


**Figure 2.** Irradiation temperature as a function of radius from the pulsar for a steady-state disk for four different accretion rates. The upper solid line is for accretion rates of  $\dot{M} > \dot{M}_{\text{crit}} = 1.45 \times 10^{-8} M_{\odot} \text{ yr}^{-1}$  that are above the Eddington luminosity and the temperature is determined with equation (21). The irradiation temperature for the lower accretion rates is determined with equation (20). We show  $\dot{M} = 10^{-8} M_{\odot} \text{ yr}^{-1}$  (second solid line),  $\dot{M} = 10^{-9} M_{\odot} \text{ yr}^{-1}$  (third solid line) and  $\dot{M} = 10^{-10} M_{\odot} \text{ yr}^{-1}$  (lower solid line). The dashed line shows the critical temperature required for the MRI to operate of  $T_{\text{crit}} = 1400 \text{ K}$ . The radius at which each of the solid line crosses the dashed line is the inner edge of a dead zone, if it forms,  $R_{\text{d,in}}$ .

We find the critical accretion rate above which the luminosity is limited by the Eddington Luminosity by solving  $L_{\text{acc}} = L_{\text{EDD}}$  to be

$$\dot{M}_{\text{crit}} = 1.45 \times 10^{-8} \left( \frac{R_{\text{p}}}{10 \text{ km}} \right) M_{\odot} \text{ yr}^{-1}. \quad (17)$$

We assume that the disk aspect ratio can be written as a power law in radius  $H \propto R^n$ , This simplifies equation (12) to read

$$\cos \phi = \frac{H}{R}(n-1). \quad (18)$$

Assuming hydrostatic equilibrium and that the disk temperature is dominated by the irradiation, we have

$$H = \frac{c_s}{\Omega} = \frac{1}{\Omega} \sqrt{\frac{\mathcal{R} T_{\text{irr}}}{\mu}}, \quad (19)$$

where  $\mathcal{R} = 8.31 \times 10^7 \text{ erg K}^{-1} \text{ mol}^{-1}$  is the gas constant and  $\mu = 2.3$  is the mean molecular weight. We take equation (11) (with  $L = L_{\text{acc}}$  defined in equation (13)) and combine it with equation (19) to write the irradiation temperature for  $L_{\text{acc}} < L_{\text{EDD}}$  as

$$T_{\text{irr}} = 1643 \left( \frac{\dot{M}}{10^{-8} M_{\odot} \text{ yr}^{-1}} \right)^{\frac{2}{7}} \left( \frac{M_{\text{p}}}{1.4 M_{\odot}} \right)^{\frac{1}{7}} \times \left( \frac{R_{\text{p}}}{10 \text{ km}} \right)^{-\frac{2}{7}} \left( \frac{R}{1 \text{ AU}} \right)^{-\frac{3}{7}} \text{ K}. \quad (20)$$

Since we find  $T_{\text{irr}} \propto R^{-3/7}$ , this gives  $H = c_s/\Omega \propto T_{\text{irr}}^{1/2} R^{3/2} \propto R^{9/7}$ . For a disk that is dominated by irradiation,  $n = 9/7$  and we use this value for the rest of the work. Similarly, for higher

accretion rates, with  $L_{\text{acc}} > L_{\text{EDD}}$ , we combine equation (11) (with  $L = L_{\text{EDD}}$  in equation (15)) with equation (19) and we find

$$T_{\text{irr,EDD}} = 1825 \left( \frac{M_{\text{p}}}{1.4 M_{\odot}} \right)^{\frac{1}{7}} \left( \frac{R}{1 \text{ AU}} \right)^{-\frac{3}{7}} \text{ K}. \quad (21)$$

In Fig. 2 we show the disk temperature as a function of radius for various accretion rates. We also show the critical temperature required for the MRI to operate. A dead zone forms when the temperature of the disk drops below this. We solve  $T_{\text{irr}} = T_{\text{crit}}$  to find the critical radius outside of which the temperature drops below that required for the MRI,

$$R_{\text{d,in}} = 1.45 \left( \frac{\dot{M}}{10^{-8} M_{\odot} \text{ yr}^{-1}} \right)^{\frac{2}{3}} \left( \frac{R_{\text{p}}}{10 \text{ km}} \right)^{-\frac{2}{3}} \times \left( \frac{M_{\text{p}}}{1.4 M_{\odot}} \right)^{\frac{1}{3}} \left( \frac{T_{\text{c}}}{1400 \text{ K}} \right)^{-\frac{7}{3}} \text{ AU}. \quad (22)$$

If, at this radius, the surface density is sufficiently high, then a dead zone forms outside of this radius. Above the Eddington limit, we solve  $T_{\text{irr,EDD}} = T_{\text{crit}}$  to find the critical inner dead zone radius

$$R_{\text{d,in,EDD}} = 1.85 \left( \frac{M_{\text{p}}}{1.4 M_{\odot}} \right)^{\frac{1}{3}} \left( \frac{T_{\text{c}}}{1400 \text{ K}} \right)^{-\frac{7}{3}} \text{ AU}. \quad (23)$$

The lower line in Fig. 4 shows the inner edge of the dead zone as a function of accretion rate. This is a combination of equation (22) for  $\dot{M} < \dot{M}_{\text{crit}}$  and equation (23) for  $\dot{M} > \dot{M}_{\text{crit}}$ . Since the inner dead zone radius does not depend upon the critical surface density it is the same in both plots. In the next Section we consider the radial location of the outer edge of the dead zone.

#### 4.2. Outer edge of the dead zone

If a dead zone is present, its outer edge is determined by the location where the surface density drops below the critical,  $\Sigma < \Sigma_{\text{crit}}$ . The viscosity of the disk is

$$\nu = \alpha \frac{c_s^2}{\Omega}. \quad (24)$$

For a steady state disk the surface density is given by

$$\Sigma = \frac{\dot{M}}{3\pi\nu} \quad (25)$$

(Pringle 1981). For our typical parameters, for an accretion rate that is not Eddington limited, this is

$$\Sigma = 26.7 \left( \frac{\dot{M}}{10^{-8} M_{\odot} \text{ yr}^{-1}} \right)^{\frac{5}{7}} \left( \frac{R_{\text{p}}}{10 \text{ km}} \right)^{\frac{2}{7}} \left( \frac{\alpha}{0.01} \right)^{-1} \left( \frac{M_{\text{p}}}{1.4 M_{\odot}} \right)^{\frac{5}{14}} \times \left( \frac{R}{1 \text{ AU}} \right)^{-\frac{15}{14}} \text{ g cm}^{-2}. \quad (26)$$

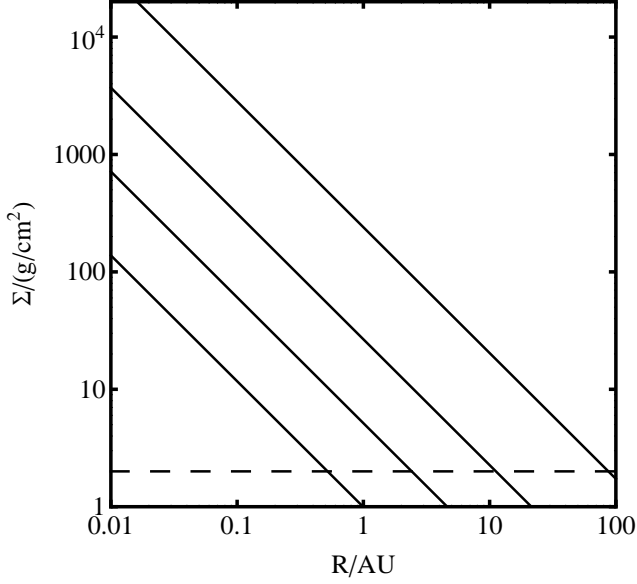


**Figure 3.** Surface density as a function of radius from the pulsar for a steady-state disk for four different accretion rates. The upper solid line is above the Eddington limit and is determined with equation (27) and shows  $\dot{M} = 10^{-7} M_{\odot} \text{ yr}^{-1}$ . The other solid lines show accretion rates below the Eddington limit that are determined with equation (26),  $\dot{M} = 10^{-8} M_{\odot} \text{ yr}^{-1}$  (second solid line),  $\dot{M} = 10^{-9} M_{\odot} \text{ yr}^{-1}$  (third solid line) and  $\dot{M} = 10^{-10} M_{\odot} \text{ yr}^{-1}$  (lower solid line). The dashed line shows the critical surface density that is ionized by external sources, of  $\Sigma_{\text{crit}} = 2 \text{ g cm}^{-2}$ . The radius at which the solid line crosses the dashed line is the outer edge of a dead zone, if it forms,  $R_{\text{d,out}}$ .

Similarly, for the case in which the luminosity is Eddington limited, we can find the surface density

$$\Sigma_{\text{EDD}} = 24.0 \left( \frac{\dot{M}}{10^{-8} M_{\odot} \text{ yr}^{-1}} \right) \left( \frac{\alpha}{0.01} \right)^{-1} \left( \frac{M_{\text{p}}}{1.4 M_{\odot}} \right)^{\frac{5}{14}} \times \left( \frac{R}{1 \text{ AU}} \right)^{-\frac{15}{14}} \text{ g cm}^{-2}. \quad (27)$$

In Fig. 3 we plot the surface density as a function of radius for various accretion rates.

We can find the radius of the outer edge of the dead zone by solving  $\Sigma = \Sigma_{\text{crit}}$ . Below the Eddington accretion rate we find

$$R_{\text{d,out}} = 1.3 \left( \frac{\dot{M}}{10^{-8} M_{\odot} \text{ yr}^{-1}} \right)^{\frac{2}{3}} \left( \frac{\alpha}{0.01} \right)^{-\frac{14}{15}} \left( \frac{R_{\text{p}}}{10 \text{ km}} \right)^{\frac{4}{15}} \times \left( \frac{M_{\text{p}}}{1.4 M_{\odot}} \right)^{\frac{1}{3}} \left( \frac{\Sigma_{\text{crit}}}{20 \text{ g cm}^{-2}} \right)^{-\frac{14}{15}} \text{ AU} \quad (28)$$

and the corresponding critical radius above the Eddington accretion rate is

$$R_{\text{d,out,EDD}} = 1.18 \left( \frac{\dot{M}}{10^{-8} M_{\odot} \text{ yr}^{-1}} \right)^{\frac{14}{15}} \left( \frac{\alpha}{0.01} \right)^{-\frac{14}{15}} \times \left( \frac{M_{\text{p}}}{1.4 M_{\odot}} \right)^{\frac{1}{3}} \left( \frac{\Sigma_{\text{crit}}}{20 \text{ g cm}^{-2}} \right)^{-\frac{14}{15}} \text{ AU}. \quad (29)$$

In Fig. 4 the upper lines show the outer edge of the dead zone that depends on both the accretion rate and the critical active layer surface density. In the next Section, we determine

whether a dead zone can exist since if  $R_{\text{d,in}} > R_{\text{d,out}}$ , then there is no region of parameter space for a dead zone and the disk is fully turbulent.

#### 4.3. Existence of a dead zone

The condition that must be satisfied for a dead zone to exist is that the surface density at the radius of the inner dead zone boundary must be larger than the critical surface density that is MRI active,

$$\Sigma(R_{\text{d,in}}) > \Sigma_{\text{crit}}. \quad (30)$$

Since the surface density in the disk increases with radius, the larger  $\Sigma_{\text{crit}}$  the less likely it is that a dead zone may form. This condition is equivalent to

$$R_{\text{d,in}} < R_{\text{d,out}}. \quad (31)$$

We consider here disk parameters for which a dead zone exists.

In Fig. (4) we show the inner and outer dead zone radii for an example with  $T_{\text{crit}} = 1400 \text{ K}$  and  $\Sigma_{\text{crit}} = 2 \text{ g cm}^{-2}$  (left) and  $\Sigma_{\text{crit}} = 0.2 \text{ g cm}^{-2}$  (right). The shaded regions show the accretion rates for which a dead zone exists and the range of radii. We find that for  $\Sigma_{\text{crit}} \gtrsim 10 \text{ g cm}^{-2}$  a dead zone does not exist for typical accretion rates. However, for a smaller critical surface density,  $\Sigma_{\text{crit}} \lesssim 10 \text{ g cm}^{-2}$ , there is a dead zone for all accretion rates. We suggest that the formation of planets around a pulsar requires a very small critical surface density. Such a low critical surface density may be difficult to achieve because cosmic rays are expected to penetrate  $\Sigma_{\text{crit}} = 200 \text{ g cm}^{-2}$ . There are several possibilities for lowering the active layer surface density. First, as described in Section 4, cosmic rays may be swept away allowing a large dead zone to form. Second, the presence of dust or polycyclic hydrocarbons can suppress the MRI. Magnetohydrodynamic simulations that include these effects find small critical surface densities (e.g. Bai 2011; Perez-Becker & Chiang 2011). Third, the inclusion of non-ideal MHD effects may decrease the amount of turbulence (e.g. Simon et al. 2013). There remains much uncertainty in the value of the active layer surface density.

We note that our model represents a steady state disk but in a real disk around the pulsar there will initially be a spreading phase before the steady state is reached. If the disk is made by the destruction of a binary companion, then, initially the material will lie at the binary orbital separation. The material spreads both inwards and outwards from there. The steady state solutions calculated in this work may only be appropriate inside of the initial binary separation radius. Depending upon the spreading rate of the disk, the dead zone may extend to the outer edge of the disk. This is especially likely for high accretion rates, early in the disk evolution. The spreading of the disk may be slowed because of the dead zone. We discuss this further in Section 5.

#### 4.4. Viscous heating

In this work so far we have not included the effect of viscous heating on the steady state disk model. We can calculate the temperature from the viscous heating

$$\sigma T_{\text{visc}}^4 = \frac{9}{8} \nu \Sigma \Omega^2. \quad (32)$$

With this, we calculate (for accretion rates below the Eddington limit) the relative temperature compared with the irradiation

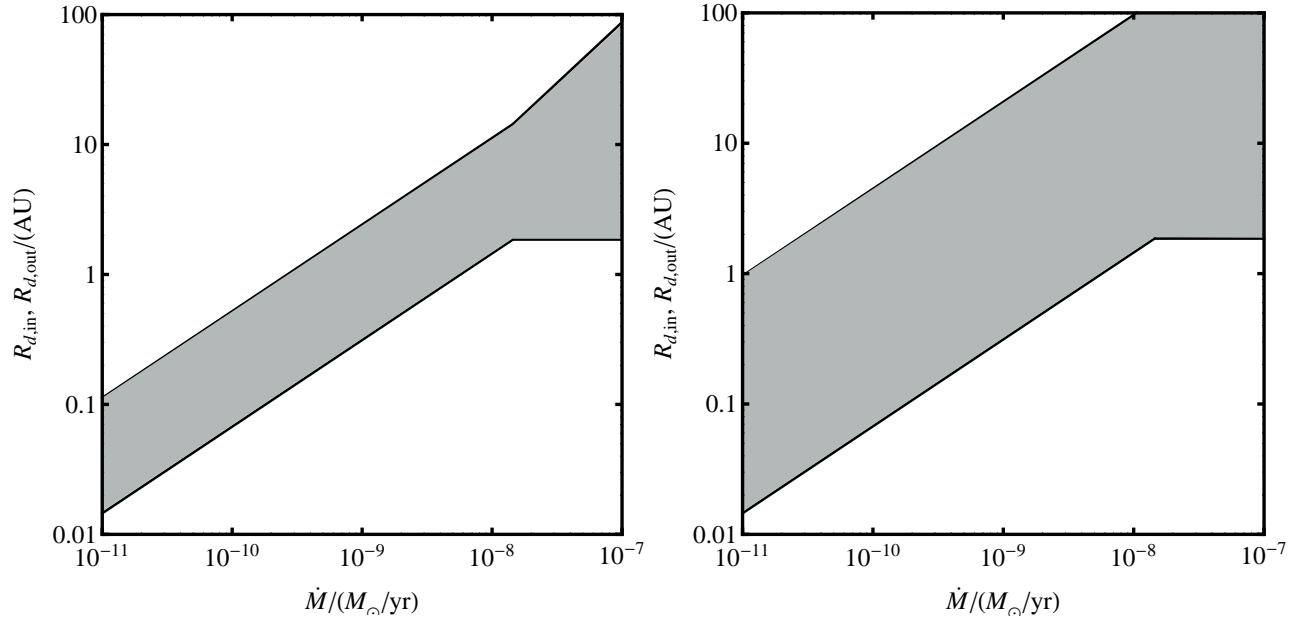


**Figure 4.** Inner edge of the dead zone,  $R_{d,in}$  (defined where  $T_{irr} = T_{crit}$ ) and the outer edge of the dead zone,  $R_{d,out}$ , (defined where  $\Sigma = \Sigma_{crit}$ ). The dead zone exists in the shaded region. We take  $T_{crit} = 1400$  K and  $\Sigma_{crit} = 2$  g cm $^{-2}$  (left) and  $\Sigma_{crit} = 0.2$  g cm $^{-2}$  (right).

tion temperature

$$\frac{T_{visc}}{T_{irr}} = 0.056 \left( \frac{\dot{M}}{10^{-8} M_{\odot} \text{ yr}^{-1}} \right)^{-\frac{1}{28}} \left( \frac{R_p}{10 \text{ km}} \right)^{\frac{2}{7}} \left( \frac{M_p}{1.4 M_{\odot}} \right)^{\frac{3}{28}} \times \left( \frac{R}{1 \text{ AU}} \right)^{-\frac{9}{28}}. \quad (33)$$

In Fig. 5 we show this ratio as a function of radius for an accretion rate of  $10^{-8} M_{\odot} \text{ yr}^{-1}$ . As seen from the above equation, this is not very sensitive to the accretion rate. Furthermore, the heating from viscous effects is much smaller than the heating due to the irradiation from the pulsar. If we were to include this heating into our steady state disk models, the temperature of the disk would increase slightly. The models we have shown here represent the maximum size of the dead zone in the absence of viscous heating.

## 5. DISCUSSION

Currie & Hansen (2007) considered the formation of pulsar planets in disks with a dead zone for two scenarios, the supernova fallback disk and the tidal disruption disk. They favor the supernova fallback disk for planet formation because they suggest that it can form the compact configuration of the observed planets. However, recent numerical simulations find that the formation of a fallback disk around a neutron star requires somewhat tuned parameters (Perna et al. 2014). As we have shown in Section 2.2, when the supernova fallback disk does form, its lifetime is very short and would not allow for planet formation. In the present work we have extended the parameter space of dead zone properties. Most importantly, we have explored the consequences of a broader range in the active layer surface density. Since two of the planets in PSR B1257+12 are in a resonance, this suggests that they formed farther out in the disk and migrated inwards. Thus, we do not require that the dead zone would be in the orbital

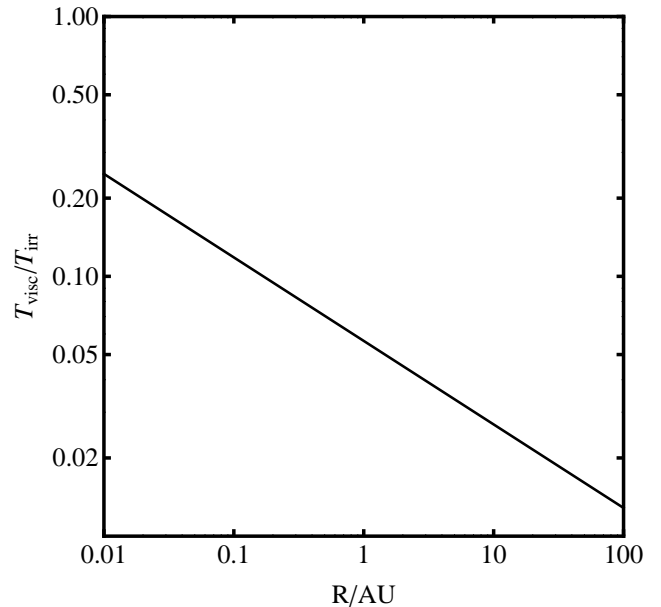


**Figure 5.** Ratio of the temperature due to viscous heating to the irradiation temperature as a function of radius from the pulsar for a steady-state disk with accretion rates  $\dot{M} = 10^{-8} M_{\odot} \text{ yr}^{-1}$ .

location of the current locations of the planets. The planets could form at an orbital radius of around 1 AU and then migrate inwards to their observed locations. Formation farther out is also possible, but this scenario should be investigated in a time-dependent disk model. Migration through a dead zone is likely to be much slower than migration through a fully viscous disk (Ward 1997; Thommes 2005; Matsumura & Pudritz 2006) and so the planets can more easily survive the migration process without being accreted on to the pulsar in the presence of a dead zone. The inner edge of the dead zone will

move inwards in time as the disk mass and accretion rate drop (see Fig. 4) and so the planets will likely remain in the dead zone throughout the disk lifetime (if the dead zone exists).

Hansen et al. (2009) used the surface density profiles from the layered disk models of Currie & Hansen (2007) to determine initial conditions for the solid material in planetary embryos for a set of N-body simulations to model the formation of planets around the pulsar PSR B1257+12. They found that the layered disk model provided a better fit to the final planetary systems because it resulted in the planets forming from a narrow annulus (this is also true in the solar system, see Hansen 2009).

Searches for debris disks around pulsars have revealed no infrared counterparts (Löhmer et al. 2004; Wang et al. 2014; Wang 2014). However, debris disks have been suggested to be around two magnetars 4U 0142+61 and 1E 2259+286 (Wang et al. 2006; Kaplan et al. 2009). Maybe the fact that planets were not found yet orbiting white dwarfs (e.g. Livio et al. 2005; Sandhaus et al. 2016; Farihi 2016), but that the surface layers of some white dwarfs show (perhaps) pollution by planets (e.g. Gänsicke et al. 2012), indicate that indeed there were no dead zones, and either planets did not form, or else they migrated all the way in through a viscous disk.

In this work we have concentrated on a steady-state disk model. However, as we have discussed in Section 4, a disk model that includes a dead zone is not in steady-state since material builds up within the dead zone. Furthermore, the dead zone will slow the rate of expansion of the disk (e.g. Hansen 2002). Material only flows outwards in a layer of surface density  $\Sigma_a$  rather than the full surface density. For small active layer surface densities, the disk will have a large extended region of low density and a compact high density dead zone region. The steady-state disk solutions described in this work are certainly adequate up to around the initial separation of the binary, but outside of that, time-dependent calculations will be required to determine the evolution. The non-monotonic surface density profile of the disk will also affect the process of planet formation and may aid the formation of a compact planetary system (Hansen 2009). In a future publication, we will investigate the time-dependent effects of such a disk model and their potential implications for pulsar planet formation.

## 6. CONCLUSIONS

We explain the small number of observed pulsar planets through a combination of two low-probability events. First, the most likely formation site is in a disk formed by the destruction of a companion star. This also explains why all the pulsar planets that we have found are around millisecond pulsars rather than young pulsars. A binary that allows for such a scenario must have an extreme mass ratio and has a very small chance of forming and surviving the supernova explosion. Second, planet formation is thought to require a dead zone, a region of low turbulence, within the protoplanetary disk. Because pulsars have a much stronger source of irradiation than a young star, the additional heating can lead to sufficient ionization that the dead zone does not form. The inner boundary of the dead zone is pushed farther out, due to the irradiation, into a region of the disk with lower surface density. A dead zone only forms if the surface density that is ionized by external sources is small,  $\Sigma_{\text{crit}} \lesssim 10 \text{ g cm}^{-2}$ .

## ACKNOWLEDGMENTS

We thank Stephen Lepp for useful conversations. This research has made use of the Exoplanet Orbit Database and the Exoplanet Data Explorer at exoplanets.org.

## REFERENCES

- Alpar, M. A., Cheng, A. F., Ruderman, M. A., & Shaham, J. 1982, *Nature*, 300, 728
- Armitage, P. J., Clarke, C. J., & Palla, F. 2003, *MNRAS*, 342, 1139
- Armitage, P. J., Livio, M., & Pringle, J. E. 2001, *MNRAS*, 324, 705
- Backer, D. C., Foster, R. S., & Sallmen, S. 1993, *Nature*, 365, 817
- Bai, X.-N. 2011, *ApJ*, 739, 50
- Bai, X.-N. & Stone, J. M. 2010, *ApJ*, 722, 1437
- Bailes, M. 1996, in *Astronomical Society of the Pacific Conference Series*, Vol. 105, IAU Colloq. 160: Pulsars: Problems and Progress, ed. S. Johnston, M. A. Walker, & M. Bailes, 3
- Bailes, M., Bates, S. D., Bhalerao, V., Bhat, N. D. R., Burgay, M., Burke-Spolaor, S., D’Amico, N., Johnston, S., Keith, M. J., Kramer, M., Kulkarni, S. R., Levin, L., Lyne, A. G., Milia, S., Possenti, A., Spitler, L., Stappers, B., & van Straten, W. 2011, *Science*, 333, 1717
- Bailes, M., Lyne, A. G., & Shemar, S. L. 1991, *Nature*, 352, 311
- Bailes, M., Lyne, A. G., & Shemar, S. L. 1993, in *Astronomical Society of the Pacific Conference Series*, Vol. 36, *Planets Around Pulsars*, ed. J. A. Phillips, S. E. Thorsett, & S. R. Kulkarni, 19–30
- Balbus, S. A. & Hawley, J. F. 1991, *ApJ*, 376, 214
- Bastian, N., Covey, K. R., & Meyer, M. R. 2010, *ARA&A*, 48, 339
- Bell, J. F., Bailes, M., Manchester, R. N., Lyne, A. G., Camilo, F., & Sandhu, J. S. 1997, *MNRAS*, 286, 463
- Benz, W., Cameron, A. G. W., Press, W. H., & Bowers, R. L. 1990, *ApJ*, 348, 647
- Bhattacharya, D. & van den Heuvel, E. P. J. 1991, *Phys. Rep.*, 203, 1
- Blaauw, A. 1961, *Bull. Astron. Inst. Netherlands*, 15, 265
- Blandford, R. D. 1993, *Pulsars as physics laboratories*
- Brandt, N. & Podsiadlowski, P. 1995, *MNRAS*, 274, 461
- Calvet, N., Muzerolle, J., Briceño, C., Hernández, J., Hartmann, L., Saucedo, J. L., & Gordon, K. D. 2004, *AJ*, 128, 1294
- Cesarsky, C. J. & Volk, H. J. 1978, *A&A*, 70, 367
- Chambers, J. E. 2010, *Icarus*, 208, 505
- Chevalier, R. A. 1989, *ApJ*, 346, 847
- Colgate, S. A. 1971, *ApJ*, 163, 221
- Currie, T. & Hansen, B. 2007, *ApJ*, 666, 1232
- Duchêne, G. & Kraus, A. 2013, *ARA&A*, 51, 269
- Farihi, J. 2016, *New Astronomy Reviews*, 71, 9
- Ford, E. B., Joshi, K. J., Rasio, F. A., & Zbarsky, B. 2000, *ApJ*, 528, 336
- Frank, J., King, A., & Raine, D. J. 2002, *Accretion Power in Astrophysics*
- Fromang, S., Terquem, C., & Balbus, S. A. 2002, *MNRAS*, 329, 18
- Fruchter, A. S., Berman, G., Bower, G., Convery, M., Goss, W. M., Hankins, T. H., Klein, J. R., Nice, D. J., Ryba, M. F., Stinebring, D. R., Taylor, J. H., Thorsett, S. E., & Weisberg, J. M. 1990, *ApJ*, 351, 642
- Gammie, C. F. 1996, *ApJ*, 457, 355
- Gammie, C. F. & Menou, K. 1998, *ApJ*, 492, L75
- Gänsicke, B. T., Koester, D., Farihi, J., Girven, J., Parsons, S. G., & Breedt, E. 2012, *MNRAS*, 424, 333
- Glassgold, A. E., Najita, J., & Igea, J. 2004, *ApJ*, 615, 972
- Han, E., Wang, S. X., Wright, J. T., Feng, Y. K., Zhao, M., Fakhouri, O., Brown, J. I., & Hancock, C. 2014, *PASP*, 126, 827
- Hansen, B. M. S., Shih, H.-Y., & Currie, T. 2009, *ApJ*, 691, 382
- Hansen, B. M. S., 2009, *ApJ*, 703, 1131
- Hansen, B. 2000, in *ASP Conf. Ser. 263, Stellar Collisions, Mergers and their Consequences*, ed. M. M. Shara (San Francisco, CA: ASP), 221
- Heger, A., Fryer, C. L., Woosley, S. E., Langer, N., & Hartmann, D. H. 2003, *ApJ*, 591, 288
- Kaplan, D. L., Chakrabarty, D., Wang, Z., & Wachter, S. 2009, *ApJ*, 700, 149
- Kennedy, G. M. & Kenyon, S. J. 2008, *ApJ*, 673, 502
- Kerr, M., Johnston, S., Hobbs, G., & Shannon, R. M. 2015, *ApJ*, 809, L11
- Konacki, M. & Wolszczan, A. 2003, *ApJ*, 591, L147
- Kratter, K. M. & Matzner, C. D. 2006, *MNRAS*, 373, 1563
- Krolik, J. H. 1991, *Nature*, 353, 829
- Lepp, S. 1992, in *IAU Symposium*, Vol. 150, *Astrochemistry of Cosmic Phenomena*, ed. P. D. Singh, 471
- Lin, D. N. C., Woosley, S. E., & Bodenheimer, P. H. 1991, *Nature*, 353, 827
- Livio, M. 2000, in *Type Ia Supernovae, Theory and Cosmology*, ed. J. C. Niemeyer & J. W. Truran, 33
- Livio, M., Pringle, J. E., & Wood, K. 2005, *ApJ*, 632, L37
- Löhmer, O., Wolszczan, A., & Wielebinski, R. 2004, *A&A*, 425, 763
- Lorimer, D. R. 2008, *Living Reviews in Relativity*, 11
- Manchester, R. N., Hobbs, G. B., Teoh, A., & Hobbs, M. 2005, *AJ*, 129, 1993
- Martin, R. G. & Lubow, S. H. 2011, *ApJ*, 740, L6
- . 2013, *MNRAS*, 432, 1616
- . 2014, *MNRAS*, 437, 682
- Martin, R. G., Lubow, S. H., Livio, M., & Pringle, J. E. 2012a, *MNRAS*, 420, 3139
- . 2012b, *MNRAS*, 423, 2718
- Martin, R. G., Tout, C. A., & Pringle, J. E. 2009, *MNRAS*, 397, 1563



- , 2010, *MNRAS*, 401, 1514
- Mason, B. D., Hartkopf, W. I., Gies, D. R., Henry, T. J., & Helsel, J. W. 2009, *AJ*, 137, 3358
- Matsumura, S. & Pudritz, R. E. 2003, *ApJ*, 598, 645
- , 2006, *MNRAS*, 365, 572
- Menou, K., Perna, R., & Hernquist, L. 2001, *ApJ*, 559, 1032
- Perez-Becker, D. & Chiang, E. 2011, *ApJ*, 735, 8
- Perna, R., Duffell, P., Cantiello, M., & MacFadyen, A. I. 2014, *ApJ*, 781, 119
- Phinney, S., Hansen, B. 1993, in *ASP Conf. Ser. 36, Planets Around Pulsars*, ed. J. A. Phillips, S. E. Thorsett, & S. R. Kulkarni (San Francisco: ASP), 371
- Podsiadlowski, P. 1993, in *Astronomical Society of the Pacific Conference Series, Vol. 36, Planets Around Pulsars*, ed. J. A. Phillips, S. E. Thorsett, & S. R. Kulkarni, 149–165
- Podsiadlowski, P. 1995, in *Astronomical Society of the Pacific Conference Series, Vol. 72, Millisecond Pulsars. A Decade of Surprise*, ed. A. S. Fruchter, M. Tavani, & D. C. Backer, 411
- Podsiadlowski, P., Pringle, J. E., & Rees, M. J. 1991, *Nature*, 352, 783
- Pringle, J. E. 1981, *ARA&A*, 19, 137
- Rasio, F. A. 1994, *ApJ*, 427, L107
- Rasio, F. A., Shapiro, S. L., & Teukolsky, S. A. 1992, *A&A*, 256, L35
- Sandhaus, P. H., Debes, J. H., Ely, J., Hines, D. C., & Bourque, M. 2016, *ArXiv e-prints*
- Shakura, N. I. & Sunyaev, R. A. 1973, *A&A*, 24, 337
- Shklovskii, I. S. 1970, *Soviet Ast.*, 13, 562
- Sigurdsson, S., Richer, H. B., Hansen, B. M., Stairs, I. H., & Thorsett, S. E. 2003, *Science*, 301, 193
- Simon, J. B., Bai, X.-N., Stone, J. M., Armitage, P. J., & Beckwith, K. 2013, *ApJ*, 764, 66
- Skilling, J. & Strong, A. W. 1976, *A&A*, 53, 253
- Stevens, I. R., Rees, M. J., & Podsiadlowski, P. 1992, *MNRAS*, 254, 19P
- Tavani, M. & Brookshaw, L. 1992, *Nature*, 356, 320
- Terquem, C. & Papaloizou, J. C. B. 2007, *ApJ*, 654, 1110
- Thommes, E. W. 2005, *ApJ*, 626, 1033
- Thorsett, S. E., Arzoumanian, Z., & Taylor, J. H. 1993, *ApJ*, 412, L33
- Thorsett, S. E. & Phillips, J. A. 1992, *ApJ*, 387, L69
- Toomre, A. 1964, *ApJ*, 139, 1217
- Umebayashi, T. & Nakano, T. 1988, *Progress of Theoretical Physics Supplement*, 96, 151
- van Haften, L. M., Nelemans, G., Voss, R., & Jonker, P. G. 2012, *A&A*, 541, A22
- Wang, Z. 2014, *Planet. Space Sci.*, 100, 19
- Wang, Z., Chakrabarty, D., & Kaplan, D. L. 2006, *Nature*, 440, 772
- Wang, Z., Kaplan, D. L., & Chakrabarty, D. 2007, *ApJ*, 655, 261
- Wang, Z., Ng, C.-Y., Wang, X., Li, A., & Kaplan, D. L. 2014, *ApJ*, 793, 89
- Ward, W. R. 1997, *Icarus*, 126, 261
- Williams, J. P. & Cieza, L. A. 2011, *ARA&A*, 49, 67
- Wolszczan, A. 1994, *Science*, 264, 538
- Wolszczan, A. 1997, in *Astronomical Society of the Pacific Conference Series, Vol. 119, Planets Beyond the Solar System and the Next Generation of Space Missions*, ed. D. Soderblom, 135
- , 2012, *New Astronomy Reviews*, 56, 2
- Wolszczan, A. & Frail, D. A. 1992, *Nature*, 355, 145
- Youdin, A. N. 2011, *ApJ*, 731, 99
- Youdin, A. N. & Lithwick, Y. 2007, *Icarus*, 192, 588
- Youdin, A. N. & Shu, F. H. 2002, *ApJ*, 580, 494
- Zhu, Z., Hartmann, L., & Gammie, C. 2009, *ApJ*, 694, 1045
- , 2010a, *ApJ*, 713, 1143
- Zhu, Z., Hartmann, L., Gammie, C. F., Book, L. G., Simon, J. B., & Engelhard, E. 2010b, *ApJ*, 713, 1134
- Zsom, A., Ormel, C. W., Dullemond, C. P., & Henning, T. 2011, *A&A*, 534, A73